Journal Pre-proof

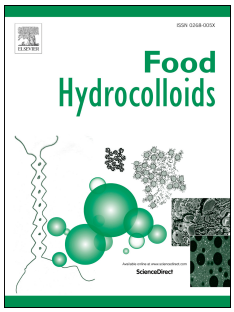

Influence of protease type and concentration on protein digestibility, physicochemical and textural properties of extruded high-moisture meat analogues

Grace Cui Fang NG, Caleb ONG, Alicia Hui Ping THENG, Dayna Shu Min ONG, Chaoyu DONG, Hui Yu SIM, Xin Yi HUA, Felicia Siew Kay NG, Jie Hong CHIANG

PII: S0268-005X(25)00870-7

DOI: https://doi.org/10.1016/j.foodhyd.2025.111910

Reference: FOOHYD 111910

To appear in: *Food Hydrocolloids*

Received Date: 9 May 2025

Revised Date: 20 August 2025

Accepted Date: 25 August 2025

Please cite this article as: Fang NG, G.C., ONG, C., Ping THENG, A.H., Min ONG, D.S., DONG, C., Yu SIM, H., Yi HUA, X., Kay NG, F.S., Hong CHIANG, J., Influence of protease type and concentration on protein digestibility, physicochemical and textural properties of extruded high-moisture meat analogues, *Food Hydrocolloids*, https://doi.org/10.1016/j.foodhyd.2025.111910.

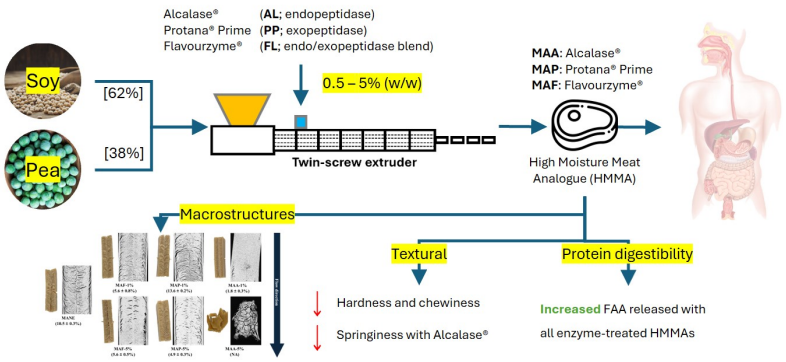

Influence of protease type and concentration on protein digestibility, physicochemical and textural properties of extruded high-moisture meat analogues

Grace Cui Fang NG * [a 1], Caleb ONG [a], Alicia Hui Ping THENG [a], Dayna Shu Min ONG [a], Chaoyu DONG [b], Hui Yu SIM [a], Xin Yi HUA [a], Felicia Siew Kay NG [a] & Jie Hong CHIANG * [a]

[a] Singapore Institute of Food and Biotechnology Innovation (SIFBI), Agency for Science, Technology and Research (A*STAR), 31 Biopolis Way, Nanos, Singapore 138669

[b] Singapore Institute of Manufacturing Technology (SIMTech), Agency for Science, Technology and Research (A*STAR), 5 Cleantech Loop, CleanTech Two Block B, Singapore 636732

[1] Present address: Food Innovation & Resource Centre, Department for Technology, Innovation and Enterprise, Singapore Polytechnic, 500 Dover Road, Singapore 139651

* Contact information for the corresponding author:

Dr Grace NG: grace_ng@sp.edu.sg

Dr Jie Hong CHIANG: chiang_jie_hong@sifbi.a-star.edu.sg

Abstract

High-moisture extrusion of plant proteins can produce meat analogues with fibrous structures and improved nutritional profiles, but replicating the meat-like texture and optimising protein digestibility remains challenging. This study investigated the effects of three proteolytic enzymes, Alcalase® (AL), Protana® Prime (PP), and Flavourzyme® (FL), added at varying concentrations (0, 0.5, 1, 2.5 and 5% w/w) on soy–pea protein-based meat analogues produced through high-moisture co-extrusion. Physicochemical and textural properties (hardness, chewiness, springiness, and degree of texturisation) were assessed alongside protein solubility, molecular weight distribution, and *in vitro* digestibility. Results indicated that low-to-moderate enzyme concentrations (0.5–1% w/w) slightly reduced hardness and chewiness while improving the fibrous structure, particularly in samples treated with FL and PP. In contrast, higher enzyme concentrations, especially with AL, induced extensive hydrolysis, resulting in fragmented extrudates and a diminished textural quality. Analysis of gastric and intestinal digesta revealed that all enzyme treatments increased soluble protein levels and the release of free amino acids compared to untreated controls. However, the specific profiles depended on enzyme selectivity. Notably, PP tended to generate higher amounts of free arginine, while AL excelled at releasing smaller peptide fragments. These findings highlight the potential to tailor textural attributes and nutritional quality in soy–pea meat analogues by selecting specific enzymes and controlling their addition, thereby paving the way for more meat-like products with enhanced protein digestibility and amino acid bioavailability.

Keywords: high-moisture meat analogues; extrusion; proteolytic enzyme; *in-vitro* digestibility; amino acids; molecular weight; texture

Abbreviations: HMMA; high-moisture meat analogues, FL; Flavourzyme®, PP; Protana® Prime, AL; Alcalase®, FAA; free amino acids

1. Introduction

Driven by the demand for healthier, more sustainable, and ethically sourced foods, meat analogues made from alternative proteins are rapidly gaining popularity (Sadowski, Talwar, Fischer, & Merritt, 2024). While offering a promising alternative to animal meat, replicating its complex texture and sensory appeal remains a major challenge. High-moisture extrusion is an advanced method for creating analogues with delicate, fibrous structures that are not achievable with low-moisture extrusion (Lee, Kim, Jeong, Choi, & Han, 2023). However, the process often results in products lacking the desired mouthfeel when compared to meat. This is largely due to the intense shear and heat involved, which can degrade proteins and negatively affect both texture and nutritional quality (Sá, Moreno, & Carciofi, 2020). Consequently, innovative food processing techniques are crucial for enhancing the quality of high-moisture meat analogues (HMMA).

The positive impact of extrusion on *in vitro* protein digestion has been well documented, with numerous studies reporting increased digestibility, highlighting its potential to enhance the nutritional value of plant-based protein products (Cutroneo, Prandi, Pellegrini, Sforza, & Tedeschi, 2024; Nadeesha Dilrukshi, Torrico, Brennan, & Brennan, 2022; Rathod & Annapure,

2016; Zhang, Liu, Ying, Sanguansri, & Augustin, 2017). The high temperatures and mechanical forces of the extrusion process, which produce extrudates, are reported to be an effective way to reduce anti-nutrient factors, such as phytic acid and trypsin inhibitors, and improve protein digestibility (Orozco-Angelino, Espinosa-Ramírez, & Serna-Saldívar, 2023). However, despite the efforts, the digestibility of meat remains superior to that of plant-based meat. In addition, the amino acid composition was affected by extrusion conditions such as moisture, pressure, temperature and other parameters, affecting specific amino acids like methionine and lysine (Alonso, Grant, Dewey, & Marzo, 2000; Hua et al., 2023; Nadeesha Dilrukshi et al., 2022).

Soy protein has been the primary focus of research on HMMA (Dou et al., 2022; Woo Choi, Ryoo, Hahn, & Choi, 2023). This is due to the desirable properties such as gelation and its ability to form an interlaced and fibrous matrix well (Schreuders et al., 2019). Concurrently, pea protein has emerged as a soy protein replacement, as peas have fewer genetically modified-related issues and are considered hypoallergenic, both of which are primary concerns for soy protein. However, structuring using pea protein for HMMA is complicated, as it has a lower gelling ability than soy protein (Schreuders et al., 2019). Combining multiple ingredients to harness their individual advantages has long been a focus in food science and technology. However, limited research has explored the use of multi-plant protein blends in the production of HMMA. Many studies use either soy (Dou et al., 2022; Woo Choi et al., 2023) or pea protein (Taghian Dinani, van der Harst, Boom, & van der Goot, 2023; Xia, Xue, Xue, Jiang, & Li, 2022) as their main protein source. There has been little Investigation into creating HMMA from a blend of soy and pea proteins until recently, where blending two protein sources can have positive effect on quality characteristics (Hua et al., 2023; Lee et al., 2023).

Enzymatic hydrolysis is a promising technique for modifying the functionality of plant proteins and enhancing their digestibility, thereby improving nutritional value. Alcalase® (AL), Flavourzyme® (FL), and Protana Prime® (PP) were selected in this study due to their well-established and mechanistically distinct proteolytic activities, allowing for a comparative assessment of their individual effects when incorporated during high-moisture extrusion. AL is a broad-specificity endopeptidase derived from *Bacillus licheniformis*, known for efficiently cleaving internal peptide bonds, particularly at hydrophobic residues, resulting in rapid protein breakdown and increased peptide solubility and digestibility (Hwang et al., 2025; Li et al., 2025; Vogelsang-O'Dwyer et al., 2023) FL, produced by *Aspergillus oryzae*, contains both endo- and exopeptidase activities, notably aminopeptidases and carboxypeptidases, enabling internal cleavage while also removing terminal residues to improve flavour and reduce bitterness (Idowu & Benjakul, 2019; Wang et al., 2025; Zhang et al., 2022) PP is a proprietary exopeptidase blend designed to liberate free amino acids from peptide termini through the actions of aminopeptidases and carboxypeptidases, thereby enhancing palatability and nutritional value through amino acid enrichment (López-Martínez, Toldrá, & Mora, 2024; Sapatinha et al., 2025; Zhang et al., 2022). These enzymes were selected to investigate how different proteolytic mechanisms, endopeptidase-only (AL), mixed endo/ exo (FL), and exopeptidase-only (PP), influence the physicochemical, structural, and nutritional properties of HMMA when applied independently during the co-extrusion process, and how they affect the digestibility of these extrudates. Recent research by Dent, Campanella and Maleky (2023) suggests that enzymatic hydrolysis of soy and chickpea protein can form insoluble aggregates suitable for texturising meat analogues. However, the impact of enzymatic hydrolysis on specific amino acids in HMMA, particularly when combined with extrusion, remains largely

unexplored. This study aims to investigate the effects of enzymatic modification during extrusion on the physicochemical, textural and nutritional (protein digestibility) properties of HMMA. This study provides a novel insight into the combined effects of enzymatic hydrolysis and extrusion.

The influence of three enzymes added at various concentrations during high-moisture extrusion of a blend of soy and pea protein on HMMA properties was investigated. AL (endopeptidase), Protana® Prime (PP, exopeptidase), and FL (a blend of endo and exopeptidase) were utilised to modify plant proteins. We hypothesised that enzymatic hydrolysis would enhance HMMA texture and nutritional quality by further increasing protein digestibility and specific amino acid accessibility.

2. Materials and methods

2.1 Materials

Soy protein concentrate (Solae Alpha® 8, USA; protein: 62.56 ± 0.13%) and pea protein isolate (NUTRALYS® F85M, France; protein: 79.01 ± 0.01%) were purchased from Connell Caldic Sdn. Bhd. (Malaysia) and Roquette Asia Pacific Pte Ltd (Singapore), respectively (Hua et al., 2023). Enzymes such as Flavourzyme® 500 MG (FL, batch: HP202599), Protana® Prime (PP, batch: QLNQ0003) and Alcalase® 2.4 L FG (AL, batch: PLN05562) were given by Novozymes. Porcine pepsin (P7012), porcine pancreatin (P7545) and porcine bile extract (B8631) were purchased from Sigma-Aldrich, Singapore. Ultrapure water purified using Milli-Q equipment (Millipore Corporation, Massachusetts, USA) was used. All other reagents and chemicals used were of analytical grade.

2.2 High-moisture extrusion of meat analogues

High-moisture meat analogues (HMMA) were produced using a laboratory, co-rotating, smooth barrel, and intermeshing twin screw extruder (Process 16 Hygienic, Thermo Fisher Scientific, Karlsruhe, Germany), with a screw diameter of 16 mm and length-diameter ratio of 40:1. From feed to exit, the extrusion screw profile comprised of: fifteen 16 mm feed screws (240 mm); twelve 4 mm mixing elements (48 mm); eight 16 mm feed screws (128 mm); ten 4 mm mixing elements (40 mm); ten 16 mm forward screws (160 mm); and one 24 mm discharge element (24 mm). The barrel consisted of a feeding zone and seven temperature-controlled zones that could be heated by an electric cartridge system and cooled by circulating water. The end of the extruder is equipped with a long die measuring 83 × 49 × 188 mm (W × H × L), with water at 80°C serving as the cooling medium.

The formulation of HMMA comprised 62.05% w/w soy protein concentrate (SPC) and 37.95% w/w pea protein isolate (PPI) in dry weight, with the protein and total amino acid profiles of these plant proteins previously reported by Hua et al. (2023). Dry materials were fed into the extruder at a feed rate of 1.72 kg/h using a gravimeter feeder (Brabender Technology GmbH, Duisburg, Germany). At the same time, 1% w/w salt solution and enzymes of different concentrations were administered into the second barrel with a peristaltic pump (Masterflex L/S, Vernon Hills, IL, USA) via an inlet port at 2.28 kg/h to achieve a moisture content (MC) of 60% w/w (wet basis) in the extruded product. Enzymes were added to the salt solution at concentrations of 0, 0.5, 1, 2.5 and 5% w/w. The temperature profile of the barrel was set at 40, 60, 80, 100, 100, 120, 120 and 120°C while the screw speed was fixed at 400 rpm. The resulting meat analogues are henceforth referred to as MANE (no enzymes added), MAF

(Flavourzyme®), MAP (Protana® Prime), and MAA (Alcalase®). For protein digestibility, unless stated otherwise, extruded samples were ground using a knife miller (GM 200, Retsch Grindomix, Germany) at 4000 rpm for 10 sec before further analysis.

2.3Physicochemical properties

Protein content was determined using Dumas combustion with an automated protein analyser (Dumatherm® N Pro, Gerhardt GmbH, Germany). The protein content was calculated with a nitrogen conversion factor of 6.25 for all samples.

The air-oven method was used to determine the moisture content (MC) of all samples. Five grams of samples were shredded, weighed into numbered pans and dried in an oven (111 Eco Line, Venticell, Germany) at 105°C for 24 hours. The weight of each pan and sample was recorded after cooling in a desiccator for an hour.

A benchtop pH meter (SevenCompact™ pH/ Ion S220, Mettler-Toledo, Switzerland) was used to measure the pH of all samples as described by Chiang, Loveday, Hardacre and Parker (2019b). The pH values were recorded after blending the samples using a high-shear mixer (T25 digital Ultra Turrax®, IKA, Germany) at 12,000 rpm, with ultrapure water at 20% w/w concentration for one minute.

2.4X-ray computed tomography (XCT)

The samples were prepared and visualised using X-ray computed tomography accordingly to Ong et al. (2025). Samples were chemically fixated in a solution containing 0.1 M phosphate

buffer (pH 7.2) with 2% formaldehyde and 3% glutaraldehyde (electron microscopy grade) for at least 8 hours, as described by Chiang et al. (2021). After fixation, samples were dehydrated through a graded series of ethanol solutions, up to 100% ethanol, to remove water. Subsequently, the samples were frozen and freeze-dried at -80°C and 0.01 mbar for 72 hours.

The dried samples were then mounted onto a carbon fibre fixture and scanned using a computed tomography scanner (X TH 225 st, Nikon, Japan). The scan parameters were set at 170 kV beam energy, 15 W of power (corresponding to an approximate spot size of 0.015 mm), and no beam hardening filter was used. Each image was captured twice to reduce noise with a low exposure of 0.7 sec and a high detector gain of 24 dB. A total of 1000 frames were captured over a full 360° of rotation. The data were reconstructed using CTPro software (version 1.1.1-b). The voxel size achieved in this scan was a high resolution of 0.04 mm. Following reconstruction, slices were manually aligned using VGStudio (version 2023.4, Volume Graphics, Germany). Three-centred representative reconstructed slices (longitudinal view) were chosen for further analysis using ImageJ (version 1.54h, National Institutes of Health, U.S). The images were subjected to thresholding to distinguish pores (dark) from the material (light). The image was then inverted, and a particle filter was applied to exclude features smaller than 300 pixels, likely representing background noise. This process allowed the isolation of pores to calculate the total pore percentage (porosity), as previously described by Ong et al. (2025).

2.5Textural analysis

The textual properties of the meat analogues were determined via a two-bite test using a texture analyser (TA.XT Plus, Stable Micro Systems, UK), as described by Chiang et al. (2019b).

Meat analogues were first cut into small pieces of 15 × 15 mm. Each sample was compressed at 1 mm/sec with a P/75 probe to 50% of its original thickness for the first bite and returned to its original position for 5 sec before being compressed again at 1 mm/sec to 50% of the first compressed thickness for the second bite. The hardness, springiness and chewiness of the HMMA were recorded from the TPA curves.

The second analysis was performed with a cutting test to assess the formation of fibrous structures. Samples of 15 × 15 mm were cut at a speed of 1 mm/sec with a craft knife adapter (A/CKB) to 75% of their original thickness. Relative to the outflow direction of the extruder, both longitudinal (lengthwise) and transverse (crosswise) cutting strengths were determined. At least six separate measurements were taken for each sample for both the TPA and cutting force tests.

2.6Protein solubility analysis

Four extraction solutions were prepared to target specific bonds: (1) P (Phosphate Buffer (PB); 0.1 M phosphate buffer consisting of KH_2PO_4 and K_2HPO_4 with a pH of 7.5, native state protein), (2) PU (PB + 8 M Urea; hydrogen bonds), (3) PD (PB + 0.05 M DTT; disulphide bonds), and (4) PS (1.5 g/100 ml SDS, hydrophobic interactions). A sample of 0.5 g was treated with 10 ml of the designated extraction solution. The mixture was agitated for 30 min at 400 rpm on a shaker (LSE™, Corning, Slovenia) to facilitate initial interaction breakdown. High shear homogenisation at 12,000 rpm for 30 sec was employed to further disrupt protein-protein interactions. The suspension was then centrifuged at 2580×g for 10 min at 25°C to separate the soluble and insoluble components. The supernatant, containing the solubilised proteins,

was transferred and centrifuged again at 10,000×g for 10 min at 25°C to remove any remaining insoluble material.

Protein concentration in the supernatant was determined using a Bradford assay performed on a cell imaging multi-mode reader (Cytation 5, BioTek, USA) at an absorbance of 595 nm. Briefly, 5 µl of the supernatant was mixed with 250 µl Bradford reagent in a 96-well plate. BSA powder served as the standard for the assay. Protein solubility was expressed as a percentage, reflecting the amount of protein solubilised by each specific extraction solution compared to the total protein content in the original sample.

2.7*In vitro* digestion and protein analysis

The *in vitro* digestion protocol used in this study followed the harmonised INFOGEST 2.0 protocol, which uses an *in vitro* static digestion model (Brodkorb et al., 2019). Electrolyte stock solutions were prepared for each digestion phase, and enzymatic activities were measured according to the assays described in the protocol. All sample digestions were performed with blanks containing 5 g of ultrapure water. Each food set and corresponding enzyme blanks were digested in triplicate to ensure representative results.

2.7.1 Oral Phase

Grounded extrudates (5 g) in 50 ml centrifuge tubes were mixed with 5 ml of simulated salivary fluid (SSF) at 37°C for 2 min. The addition of α-amylase was omitted in this phase.

2.7.2 Gastric phase

For the gastric phase, the oral bolus was mixed with SGF-containing porcine pepsin (2000 U/ml of digesta); pH was adjusted to 3.0 ± 0.1 and incubated at 37°C for 120 min on a rotary wheel at 40 rpm (Bibby Scientific™ Stuart™ Rotator SB3, UK). Gastric digestion was terminated by increasing the pH to 7.0 with 5 M NaOH to inactivate pepsin. Samples collected at this phase had their digestion terminated at pH 8.0 with 5M NaOH to inactivate pepsin instead. The addition of RGE lipase was omitted in this phase because lipids were not the primary focus of investigation. Digested HMMA collected at the gastric phase were labelled as MAF-G (FL, Gastric), MAP-G (PP, Gastric), and MAA-G (AL, Gastric).

2.7.3 Intestinal phase

For the intestinal phase, at the end of 120 min of gastric digestion, the digesta was mixed with SIF comprising porcine pancreatin (100 U trypsin activity/ml of digesta) and porcine bile extract (10 mM final concentration), with pH adjusted to 7.0 ± 0.1 and was incubated and agitated under conditions similar to the gastric phase. Intestinal digestion was stopped by adding Pefabloc®SC (5 mM final concentration). The digesta samples were centrifuged at 13000×g (fixed angle 35° rotor) for 15 min before the supernatant and residue were separated and stored at -80°C for further analysis. Digested HMMA collected at the intestinal phase were labelled as MAF-I (FL, Intestinal), MAP-I (PP, Intestinal), and MAA-I (AL, Intestinal).

2.7.4 Soluble protein quantification by Bradford assay

Prior to the Bradford assay, the supernatant of the gastric and intestinal digesta was filtered through a 0.45 µm polyethersulfone (PES) syringe filter. The quantification of soluble proteins

in the supernatants was conducted utilising the Bradford protein assay as described in Section 2.6.

2.7.5 Free amino groups quantification by o-phthaldialdehyde (OPA) assay

Prior to the o-phthaldialdehyde (OPA) assay, the supernatant of the gastric and intestinal digesta was filtered through a 0.45 µm polyethersulfone (PES) syringe filter. The amount of small peptides (approximately <6 kDa) and free amino groups released after *in vitro* digestion were quantified by the OPA assay according to Torcello-Gómez et al. (2020) with modifications. 166 µl of 5% w/v trichloroacetic acid was added to 100 µl of digesta filtrate and centrifuged at 10,000×g for 30 min. This was done to remove the longer peptides and prevent interference in the analysis. A standard curve was determined using L-serine at different concentrations. 200 µl of freshly prepared OPA working reagent was added to 10 µl of either L-serine standard, supernatant or digestion blank. Using a 96-well UV-transparent polystyrene plate, triplicate absorbance measurements were read at 340 nm in a microplate reader (BioTek Cytation 5, Agilent Technologies, California, USA) after incubation for 15 min at room temperature in a dark environment.

2.7.6 Molecular weight distribution

SDS-PAGE analysis was performed on undigested as well as digested gastric and intestinal samples in accordance with the method detailed by Lin et al. (2022) with modifications. For the processing of undigested samples, a portion of the ground sample (10 mg) was combined with 1 ml of buffer solution containing (0.5 M Tris, 2.0% SDS, 0.03% DTT, pH 6.8). To facilitate the separation of the protein subunits in the undigested samples, a reducing agent (500 mM

dithiothreitol, NuPAGE™ Sample Reducing Agent from Thermo Fisher Scientific, Waltham, USA) was added. The mixture was gently agitated for three hours at room temperature. Conversely, the digesta samples did not undergo this treatment involving the reducing agent. Instead, the digesta samples were briefly heated at 95℃ for 5 min, combined with the same buffer solution in an equal 1:1 (v/v) ratio. The resulting mixture was then gently agitated at room temperature for three hours and subsequently heated at 95°C for an additional 5 min and cooled. Prior to loading, samples were additionally diluted at a 1:2 and 1:4 volume ratio for undigested and gastric samples, respectively.

Equal volumes (10 µl) of prepared solution were loaded onto precast gels (NuPAGE 10% Bis-Tris Midi Gel polyacrylamide, Thermo Fisher Scientific, Carlsbad, USA). A molecular weight marker (PageRuler Plus Pre-Stained Protein Ladders (10-250 kDa), Thermo Fisher Scientific, Waltham, USA) was loaded on each gel. After loading, the electrophoresis was performed using a SureLock™ Tandem Midi Gel system (Thermo Fisher Scientific, Carlsbad, USA) at 120 V for 70 min. The gels were stained with InstantBlue™ Protein Stain (Sigma Aldrich, Singapore) for 40 min (Kang, Gho, Suh, & Kang, 2002). Images were captured with an iBright™ FL1500 Imaging System (Invitrogen™, Life Technologies Holdings, Singapore).

2.7.7 Free amino acid composition

Free amino acids were determined using an L-8900 amino acid analyser (Hitachi, Japan) according to the method described by Lin et al. (2022), with modifications. Briefly, the supernatant of the *in vitro* digested HMMA was mixed with 5% sulfosalicylic acid in a ratio of 4:1 (v/v, supernatant:sulfosalicylic acid) to precipitate the proteins. The sample mixture was

centrifuged at 13,000×g for 30 min. The supernatant was extracted and filtered through 0.22 µm filters before HPLC analysis.

2.8Data analysis

All measurements were performed in triplicate, and results are reported as mean values ± standard deviation (SD). Statistical analysis was performed using Minitab 17 software (Minitab Inc., USA). One-way analysis of variance (ANOVA) with Tukey's post-hoc test for pairwise comparisons ($p \leq 0.05$) was used to assess significant differences between samples. Data visualisation was performed using RStudio 2023.12.1 (PBC, Boston, Massachusetts, USA).

3. Results and discussion

3.1Physicochemical properties

The protein content, moisture content (MC), and pH of the HMMA (both with and without enzymes added during extrusion) were evaluated (**Table 1**). The MC for all HMMA samples ranged between 54.43 ± 0.39% and 57.76 ± 0.53% (results not shown), as the extrusion processing conditions remained constant throughout. The working pH and temperature range for Flavourzyme® (FL), Protana® Prime (PP), and Alcalase® (AL) were pH 4-8, pH 6-7, pH 6.5-10, and 30-65°C, 20-60°C, and 60-75°C, respectively, based on the specification listed by the manufacturer. It was expected that there would be changes in the pH and protein content of the HMMA after extrusion, as these enzymes could function optimally in the first two zones of the extrusion process based on the barrel cooking temperature profile used.

Based on cleavage site specificity, proteases can be categorised as endo- or exopeptidases (Vogelsang-O'Dwyer, Sahin, Arendt, & Zannini, 2022). Endopeptidases cleave internal peptide bonds, producing peptides of varying lengths (Tacias-Pascacio et al., 2020). AL is a serine endopeptidase that primarily cleaves internal peptide bonds within the polypeptide chain, typically at the carboxyl side of large hydrophobic amino acids such as phenylalanine and tyrosine, leading to the generation of smaller peptides (Rawlings, Barrett, & Bateman, 2012). In contrast, exopeptidases like PP primarily act on the terminal ends of peptides to release single amino acids, commonly leucine, alanine, and arginine, or short fragments, such as dipeptides or tripeptides (Nandan & Nampoothiri, 2020). FL cleaves internal peptide bonds, including at sites with glutamic acid or tyrosine, while its exopeptidase activity liberates N-terminal amino acids like glutamine, leucine, and phenylalanine, enabling a more extensive and synergistic hydrolysis (Berends, Appel, Eisele, Rabe, & Fischer, 2014; Gu et al., 2022). These distinct mechanisms of protein breakdown likely contributed to the observed differences in the physicochemical properties of the resulting HMMA.

The protein content of the HMMA generally showed little or no significant difference (**Table 1**). However, it was observed that the protein content of MAA decreased as the enzyme concentration increased, accompanied by changes in the physical appearance of HMMA, as shown in **Figure 1**. Intact HMMA was only observed at lower enzyme levels, while the highest concentration (i.e., 5% w/w) resulted in fragmented extrudates. Enzymatic hydrolysis of proteins resulted in proteolysis, leading to a subsequent decrease in protein molecular weight (Razavizadeh, Alencikiene, Vaiciulyte-Funk, Ertbjerg, & Salaseviciene, 2022). This reduction lowered the viscosity of the slurry, leading to decreased shear stress during extrusion (Wittek, Walther, Karbstein, & Emin, 2021). Given the critical role of viscosity in the physical and

chemical transformations within the extruder barrel, the changes in viscosity likely contributed to the observed decrease in protein content in MAA.

A decrease in the pH of HMMA with increasing enzyme concentration (**Table 1**) was also likely attributed to protein hydrolysis. This process releases amino groups, altering the pH of the food matrix depending on the specific protein and protease involved (Camacho, González-Tello, Páez-Dueñas, Guadix, & Guadix, 2001). This phenomenon aligned with Chiang, Eyres, Silcock, Hardacre and Parker (2019a), who attributed the pH decrease in beef bone hydrolysates to proton exchange between deionised carboxyl and amino groups during enzymatic hydrolysis.

[Insert **Table 1**]

3.2Visual images, macrostructures and porosity

Figure 1 shows the internal structure of HMMA with and without enzyme addition at 1% and 5% w/w. These concentrations were selected to effectively represent the initial onset and the maximal impact of enzymatic effects on the HMMA structure, respectively. Visually, no significant structural differences were observed between MANE, MAF-1% and MAP-1%, while MAA-1% displayed markedly smaller and thinner fibres. At 5% w/w enzyme concentration, both MAF and MAP exhibited slightly finer fibres compared to their 1% counterparts, suggesting an enzyme-mediated texturisation effect (Dai & An, 2024). However, MAA-5% produced fragmented extrudate (**Figure 1**) due to a phenomenon known as ‘flashing’, where rapid water vaporisation upon extrusion causes product disintegration (Schmid, Farahnaky, Adhikari, & Torley, 2022).

In addition to visual analysis, X-ray computed tomography (XCT) was employed to characterise the HMMA internal structure (**Figure 1**). Pores appeared as black spaces within the white protein-dense matrix. MANE exhibited a porosity of 10.5 ± 0.3%, characterised by thin black spaces. MAP-1% demonstrated increased porosity (13.6 ± 0.2%) with numerous larger pores. Conversely, MAF-1% showed reduced porosity (5.6 ± 0.8%), indicating a denser structure with fewer pores. MAA-1% displayed the lowest porosity (1.8 ± 0.3%), which also signifies a highly dense material. Both MAF-5% and MAP-5% exhibited low porosities (5.6 ± 0.5% and 4.9 ± 0.3%, respectively), suggesting a loss of porous structure at higher enzyme concentrations. These findings indicate that enzyme concentration has a significant influence on HMMA structure, particularly between 1% and 5%. Porosity could not be calculated for MAA-5% due to sample fragmentation caused by flashing during extrusion, which likely affected the distribution of water-rich components within the matrix.

[Insert **Figure 1**]

3.3 Textural properties

The hardness, springiness, chewiness, and degree of texturisation (DT) of all HMMA samples are shown in **Table 1**. The hardness, springiness, and chewiness of all enzyme-treated HMMA were significantly lower than those of MANE. For MAF, MAP, and MAA samples, the hardness and chewiness decreased markedly at 0.5% w/w enzyme concentration, followed by a slight increase at 1% w/w before declining further at 2.5% and 5% w/w. No significant difference was observed in springiness for all samples except for MAA, which decreased significantly at 2.5 and 5% w/w concentrations.

Enzymatic hydrolysis alters the functional properties of proteins through structural modifications (Wouters, Rombouts, Fierens, Brijs, & Delcour, 2016). This process reduces molecular weight, increases hydrophobicity, and releases ionisable groups, impacting properties like gelation, water/ fat-holding capacity, and emulsification. Extrusion intensifies these effects due to heat and shear (Zhou, Liu, & Feng, 2017). **Table 1** shows improved DT for MAF-1% and MAP-1%, indicating enhanced HMMA structure. However, at higher enzyme concentrations (≥2.5% w/w), textural properties (hardness, springiness, chewiness, and DT) were reduced, suggesting an optimal enzyme dose between 1% and 2.5%.

The textural properties of MAA at 2.5% and 5% w/w enzyme concentrations were further reduced due to extensive protein hydrolysis. AL, as an endopeptidase, cleaves proteins in the middle of the amino acid chains (Rawlings et al., 2012), generating larger peptides compared to exopeptidases (Tacias-Pascacio et al., 2020). However, endopeptidases can cleave proteins regardless of the terminal peptide linkages, which provides a bigger range of cleaving sites. As a result, the proteolysis of proteins in MAA may have been more extensive, leading to a greater reduction in the molecular weight of the proteins compared to other enzymes. Smaller peptides impair protein gelling due to reduced molecular weight and increased charged groups (Zhu, Yang, & Chen, 2024). Gelation is crucial for extrusion-based texturisation, contributing to the formation of anisotropic structures in meat analogues (Webb, Dogan, Li, & Alavi, 2023; Zhang et al., 2022). Thus, the reduced gelling capacity of AL-hydrolysed proteins likely contributed to the poorer textural properties of MAA at higher enzyme concentrations.

3.4 Chemical bond elucidation

[Insert **Figure 2**]

The effects of different enzymes on the amount of protein solubilised from HMMA were assessed using four extracting solutions: phosphate buffer (P), disulfide bond-disrupting (PD), hydrogen bond-disrupting (PU), and hydrophobic interaction-disrupting (PS) solutions (**Figure 2**). The highest protein solubility was consistently observed under urea treatment (PU), indicating that hydrogen bonds play a dominant role in the formation and stabilisation of the HMMA structure (Chiang et al., 2019b). However, enzyme treatment did not significantly alter this stabilisation pattern. While minor solubility changes were observed with some enzymes under DTT (PD) and SDS (PS) extractions, these variations were considerably less pronounced than those observed with urea.

Under DTT (PD) extraction, MAF-1% exhibited a slight decrease in solubility, whereas MAP-1% showed a corresponding increase. These contrasting trends can be attributed to the differing proteolytic mechanisms of the enzymes applied during extrusion. PP, composed predominantly of exopeptidases, cleaves amino acids from the N- and C-termini of the peptides while largely preserving the core protein structure. This limited proteolysis may expose previously buried cysteine residues, thereby increasing the availability of free sulfhydryl (-SH) groups. During high moisture extrusion, these exposed thiols can readily oxidise to form disulfide bonds, leading to increased protein aggregation that is then effectively disrupted by DTT, resulting in the increased solubility observed in MAP-1%. (Guo, Zhao, Yang, Li, & Yu, 2022; Hülsebusch, Heyn, Amft, & Schwarz, 2025). In contrast, FL exhibits both endo- and exopeptidase activities and has been shown to generate shorter peptides

461 through extensive internal cleavage, resulting in fragmented peptides that have diminished
462 capacity for peptide-peptide alignment and crosslinking (Carrera-Alvarado, Toldrá, & Mora,
463 2023; López-Martínez et al., 2024). This mechanism may explain the decreased insolubility of
464 MAF-1% under DTT, where fragmented peptides do not readily reform extensive disulfide
465 bonds during extrusion, yielding an extrudate with reduced aggregation and higher DTT-
466 soluble protein (Ji et al., 2023). These findings suggest that the type of proteolysis, terminal-
467 specific vs. internal cleavage, not only influences protein solubility but also modulates the
468 formation and stability of disulfide-linked aggregates during HMMA texturisation.
469
470 A significantly higher amount of protein was solubilised from MAA compared to other
471 samples using the hydrophobic interaction-disrupting (PS) solution. This aligns with studies
472 reporting increased surface hydrophobicity following AL treatment. Wang, Cheng, Wang and
473 Yang (2022) reported an initial increase in hydrophobicity after 1 min of treatment, followed
474 by a reduced increase with longer durations. Shahbal, Jing, Bhandari, Dayananda and Prakash
475 (2023) also reported increased hydrophobicity in hemp protein, emphasising the role of
476 protein type and structure in AL's ability to expose hydrophobic groups. However, an
477 imbalance of hydrophobic interactions, without sufficient hydrophilic counterparts, can
478 negatively impact texturisation (Zhang et al., 2023). AL is a subtilisin-type serine protease that
479 preferentially cleaves peptide bonds after large hydrophobic amino acid residues, such as
480 leucine and phenylalanine, exposing these regions, which then interact and aggregate during
481 extrusion, strengthening hydrophobic interactions and reducing solubility under PS
482 conditions (Khushairay, Ayub, & Babji, 2014; Nourmohammadi, SadeghiMahoonak, Alami, &
483 Ghorbani, 2017; Tacias-Pascacio et al., 2020). The effective cleavage by AL exposed previously
484 buried hydrophobic regions within the protein structure. These regions then aggregated to

minimise contact with water, resulting in increased hydrophobic interactions between protein molecules, which compromised the texture, as seen in Section 3.3 (Khushairay et al., 2014).

3.5 Protein digestibility

3.5.1 Soluble protein quantification by Bradford assay

[Insert **Figure 3**]

Figure 3 illustrates the soluble protein content in HMMA digesta after *in vitro* gastric and intestinal digestion. Significant concentration-dependent effects were observed in gastric digesta within each enzyme type, but not in intestinal digesta. In gastric digesta, MAF-5% exhibited significantly higher soluble protein compared to lower FL concentrations, while MAP-0.5% showed significantly lower soluble protein than higher PP concentrations.

Comparing enzymes at the same concentration, MAF-G exhibited the highest soluble protein, while MAP-G had the lowest amount after gastric digestion. This reflects broader internal cleavage by FL than the more limited terminal activity of PP (see Sections 3.3 and 3.4), which influenced pepsin accessibility (López-Martínez et al., 2024; Pismag, Polo, Hoyos, Bravo, & Roa, 2024; Santos-Sánchez et al., 2024; Wang et al., 2017).

In the intestinal phase, soluble protein levels converged across samples, consistent with the broad proteolytic activity of pancreatic enzymes that degrade peptides regardless of initial

treatment (Brodkorb et al., 2019; Minekus et al., 2014). Similar normalisation trends have been reported for plant-based proteins after complete *in vitro* digestion (Luz et al., 2024).

3.5.2 Free amino groups quantification by OPA assay

[Insert **Figure 4**]

Figure 4 shows the quantification and comparison of free amino groups across different enzyme types and concentrations in digested HMMA. The enzyme type had minimal impact on the release of free amino groups and small peptides. Following gastric digestion, no significant differences were detected across any enzyme types or concentrations. However, an exception was found in MAP-G at 5% w/w, which exhibited a significantly lower release of amino groups compared to MAA-G. The lower amino group release in MAP-G may result from peptide reaggregation during extrusion, reducing pepsin accessibility. In contrast, MAA-G yielded more fragments available for hydrolysis, consistent with its stronger cleavage activity (see Section 3.3).

Consistent with earlier findings, endopeptidases (AL, FL) generated more peptides than the exopeptidase (PP) (Ceuleers et al., 2016; van der Velden & Hulsmann, 1999). This agrees with previous studies reporting higher hydrolysis with AL and FL than with PP (Carrera-Alvarado, Toldrá, & Mora, 2024).

Hydrolysis duration influences peptide and amino group release. AL has been shown to achieve higher hydrolysis than FL at shorter dwell times (<100–120 min) (Dent et al., 2023;

Meinlschmidt, Sussmann, Schweiggert-Weisz, & Eisner, 2016), while FL may outperform AL with longer durations (Singh, Paul, & Goel, 2024). Since enzymes were co-extruded rather than applied for controlled durations, residence time in the barrel likely determined the observed AL–FL trends.

Overall, intestinal digestion minimised treatment differences, mirroring soluble protein results. This reinforces the conclusion that pancreatic enzymes largely override structural variations introduced during extrusion.

3.5.3 Molecular weight distribution

[Insert **Figure 5**]

Figure 5 reveals the molecular weight distributions of undigested HMMA, gastric and intestinal digesta of HMMA, specifically HMMA with no enzymes added and HMMA co-extruded with FL, PP, and AL. Undigested MANE displayed faint bands corresponding to native subunits of soy and pea proteins (He, Liu, Zhao, Wang, & Chen, 2014). MANE also displayed a higher intensity in the background between 10–25 kDa compared to the enzyme-treated samples (MAF, MAP, and MAA). This might be due to low-molecular-weight proteins, such as Bowman-Birk inhibitors (~8-10 kDa) and other protease inhibitors. In addition, protein aggregation during extrusion can cause peptide fragments to become more dye reactive as well, suggesting that the use of enzymes reduces this aggregation within the peptide band (Kennedy, 1998; Wang, 2005).

554 Undigested MAF exhibited a broad range of peptide sizes, demonstrating that combined exo
555 and endopeptidase activities produce diverse fragments (Rong et al., 2013). Undigested MAP
556 primarily displayed molecular-weight bands between 25 and 70 kDa, suggesting that
557 exopeptidase activity, which sequentially removes amino acids from peptide ends, leads to
558 the generation of smaller peptides over time (Adler-Nissen, 1986). As amino acids average in
559 length from 75 to 135 Da, they cannot be identified in **Figure 5a** due to the method's lower
560 limits. Undigested MAA showed similar peptide bands to those of undigested MAF, but with
561 more intense lower peptide bands around 10– 15 kDa. This reflects the action of
562 endopeptidase, yielding larger peptide fragments (Zhu, Zhou, & Qian, 2006). These
563 observations can also be due to FL and AL having produced a higher degree of hydrolysis than
564 PP.
565
566 The differences between the enzymes at a 1% concentration were minimal, and more
567 pronounced variations in the molecular weight distribution were observed at a 5%
568 concentration. To supplement this, the molecular weight distribution at a 5% concentration
569 was added for comparison, as shown in **Figure 5b**. At 5% enzyme concentration, more intense
570 and differentiated bands were observed across samples, indicating higher hydrolysis. MAF
571 and MAP at the 5% enzyme concentration showed more intense peptide bands with the same
572 distribution as those at 1%, suggesting higher hydrolysis activity with higher enzyme
573 concentration. This is evidenced by the more intense unmigrated peptide bands, larger than
574 190 kDa (i.e., at the edge of the separation gel), compared to those with enzyme addition at
575 5%, suggesting that there were more large peptides with 1% enzyme addition. MAA-5%
576 exhibited distinct bands around 50 kDa, suggesting accumulation of specific peptide
577 fragments due to AL's cleavage preference. The presence of a stronger peptide intensity

compared to 1% could indicate the strong and preferential endopeptidase action in AL, resulting in the formation of larger peptides around that size (Rao, Bajaj, & Mann, 2020).

The molecular weight distribution of the gastric digesta of digested MANE, MAF, MAP and MAA was illustrated in **Figure 5c**. MANE exhibited a lighter lane background and fewer peptide bands during the gastric phase compared to MAF, MAA, and MAP. This is likely due to large peptide fractions that were not cleaved (>190 kDa), unlike those that were enzymatically treated, which showed intense backgrounds and dark peptide bands. It is also reported that plant-based meat analogues are more resistant to digestion within the gastric phase (Chen et al., 2022). MAF and MAA exhibited less intense background lanes, whereas MAP showed higher background intensity between 25 and 80 kDa, likely from uncleaved peptide cores resisting pepsin digestion. These findings reinforce earlier results showing reduced digestibility in PP-treated samples during the gastric phase. This underscores the importance of the intestinal phase for comprehensive peptide fragmentation, as clearer bands were observed during this phase, where bile salts and higher pH enhance protein unfolding and enzyme accessibility (Minekus et al., 2014). Studies by Egger et al. (2017) and Dupont et al. (2010) also indicate that significant protein degradation predominantly occurs during the intestinal phase, emphasising its critical role in digestion.

The molecular weight distribution of the intestinal digesta of digested MANE, MAF, MAP and MAA was also illustrated in **Figure 5c**. No significance in terms of background or peptide bands intensity can be observed for all samples post-intestinal digestion. These bands were largely normalised, consistent with the homogenising effects of pancreatic enzymes. Extensive

proteolysis across all samples led to minimal differences in final peptide profiles, as also observed in free amino group and FAA measurements.

3.5.4 Free amino acids

[Insert **Table 2**]

The release of free amino acid (FAA) after *in vitro* protein digestion of HMMA co-extruded with 1% w/w enzymes is shown in **Table 2**. All enzyme treatments significantly enhanced FAA release compared to MANE. However, differences between enzymes were minor, except for proline and arginine. Despite these variations, the overall release of total FAA, indispensable FAA, and dispensable FAA did not differ significantly between enzyme types. This convergence is consistent with the extensive hydrolytic capacity of intestinal digestive enzymes, which tend to normalise digestion outcomes across treatments (Mulet-Cabero et al., 2020; Xin, Zhao, Tian, & Li, 2023). The SDS-PAGE results (**Figure 5**) corroborate this, showing normalised peptide band patterns after intestinal digestion, despite having different intensities in the undigested and gastric-digested samples.

The addition of enzymes resulted in considerable protein hydrolysis, releasing an increased amount of FAA, with leucine, lysine, and phenylalanine showing the highest levels among indispensable FAA (**Table 2**). Legume proteins are generally higher in leucine and phenylalanine but deficient in sulfur-containing amino acids such as cysteine and methionine (Day, 2013; Herreman, Nommensen, Pennings, & Laus, 2020; Hua et al., 2023), a pattern that was also evident across all digesta.

Among individual amino acids, MAF showed significantly higher proline release than MAP and MAA, while arginine release was notably higher in MAP compared to MAA. The distinct release patterns of proline among the enzymes are highly indicative of their specific cleavage preferences. Specifically, exopeptidases like PP are known to be less effective at cleaving peptide bonds adjacent to proline residues (Kumar & Takagi, 1999), leading to their minimal impact on proline release. AL exhibits limited capacity to hydrolyse bonds immediately preceding or following proline (Gupta, Beg, & Lorenz, 2002). The prolyl endopeptidases in FL possess a broader specificity and are highly efficient at cleaving peptide bonds involving proline (Maeda et al., 2016; Zhang et al., 2023). This unique enzymatic characteristic of FL directly explains the significantly higher release of proline from HMMA observed in **Table 2**, in contrast to the unchanged proline levels seen with MAP and MAA. The significant disparity in basic-type FAA release, particularly for arginine, between MAP (PP-treated) and MAA (AL-treated) is a direct consequence of their distinct enzyme specificities and preferred cleavage sites, which has been discussed in section 3.1.

Overall, enzyme-assisted extrusion enhanced FAA release compared to untreated controls, but the final profiles were largely equalised by intestinal digestion. This suggests that while enzyme choice can shape early digestion kinetics (e.g., proline or arginine release), the ultimate amino acid availability is primarily governed by the strong proteolytic action of intestinal digestive enzymes.

4. Conclusion

This study demonstrates how targeted enzymatic modification can be harnessed to improve the textural and nutritional properties of soy–pea-based HMMA. Lower enzyme concentrations supported the formation of desirable fibrous structures and moderately reduced hardness and chewiness. Enzymes containing both endo- and exopeptidase activities (FL) or exopeptidase activity (PP) proved beneficial in refining texture without substantial loss of product integrity. However, very high enzyme levels, most notably with AL, led to over-hydrolysis, fragmentation, and poorer textural quality. *In vitro* digestion results showed that each enzyme significantly increased both soluble protein and FAA release, albeit with different peptide and amino acid profiles. These enzymatic pathways can thus be strategically deployed to achieve specific goals, from improving mouthfeel to enhancing digestibility or boosting essential amino acid content. Future research could optimise residence time and explore sequential or combination treatments, thereby further refining the interplay between structure formation, protein functionality, and overall palatability in meat analogues. Ultimately, this enzymatic approach offers a versatile toolkit for product developers aiming to bridge the sensory and nutritional gaps between plant-derived and conventional animal-based proteins.

Acknowledgement

This research was funded by the A*STAR BMRC (Biomedical Research Council) on SFS-2 IAF-PP Future Foods: Alternative Proteins: H20H8a0002 and was awarded to Jie Hong Chiang.

Declaration of interest

The authors declare that they have no conflict of interest.

Author contributions

Grace NG: Methodology, Formal analysis, Investigation, Writing-Original, Writing-Review & Editing, Visualisation. **Kian Siang ONG, Alicia THENG, Dayna ONG, Hui Yu SIM, Xin Yi HUA, Felicia NG:** Methodology, Formal analysis, Investigation, Writing-Review & Editing. **Chaoyu DONG:** Methodology, Formal analysis, Investigation. **Jie Hong CHIANG**: Conceptualisation, Methodology, Writing-Review & Editing, Supervision, Project administration, Funding acquisition.

References

Alonso, R., Grant, G., Dewey, P., & Marzo, F. (2000). Nutritional assessment in vitro and in vivo of raw and extruded peas (Pisum sativum L.). *Journal of Agricultural and Food Chemistry*, *48*(6), 2286-2290. https://doi.org/10.1021/jf000095o

Berends, P., Appel, D., Eisele, T., Rabe, S., & Fischer, L. (2014). Performance of enzymatic wheat gluten hydrolysis in batch and continuous processes using Flavourzyme. *LWT - Food Science and Technology*, *58*(2), 534-540. https://doi.org/https://doi.org/10.1016/j.lwt.2014.03.035

Brodkorb, A., Egger, L., Alminger, M., Alvito, P., Assunção, R., Ballance, S., Bohn, T., Bourlieu-Lacanal, C., Boutrou, R., Carrière, F., Clemente, A., Corredig, M., Dupont, D., Dufour, C., Edwards, C., Golding, M., Karakaya, S., Kirkhus, B., Le Feunteun, S., . . . Recio, I. (2019). INFOGEST static in vitro simulation of gastrointestinal food digestion. *Nature Protocols*, *14*(4), 991-1014. https://doi.org/10.1038/s41596-018-0119-1

Camacho, F., González-Tello, P., Páez-Dueñas, M.-P., Guadix, E.-M., & Guadix, A. (2001). Correlation of base consumption with the degree of hydrolysis in enzymic protein hydrolysis. *Journal of Dairy Research*, *68*(2), 251-265. https://doi.org/10.1017/S0022029901004824

Carrera-Alvarado, G., Toldrá, F., & Mora, L. (2023). Potential of dry-cured ham bones as a sustainable source to obtain antioxidant and DPP-IV inhibitory extracts. *Antioxidants*, *12*(6), 1151. https://www.mdpi.com/2076-3921/12/6/1151

699 Carrera-Alvarado, G., Toldrá, F., & Mora, L. (2024). Effect of thermal pretreatment and
700 gastrointestinal digestion on the bioactivity of dry-cured ham bone enzymatic
701 hydrolyzates. *Food Research International*, *188*, 114513.
702 https://doi.org/https://doi.org/10.1016/j.foodres.2024.114513

703 Ceuleers, H., Van Spaendonk, H., Hanning, N., Heirbaut, J., Lambeir, A.-M., Joossens, J.,
704 Augustyns, K., De Man, J., Meester, I., & De Winter, B. (2016). Visceral hypersensitivity
705 in inflammatory bowel diseases and irritable bowel syndrome: The role of proteases.
706 *World Journal of Gastroenterology*, *22*, 10275.
707 https://doi.org/10.3748/wjg.v22.i47.10275

708 Chen, D., Rocha-Mendoza, D., Shan, S., Smith, Z., García-Cano, I., Prost, J., Jimenez-Flores, R.,
709 & Campanella, O. (2022). Characterization and cellular uptake of peptides derived
710 from in vitro digestion of meat analogues produced by a sustainable extrusion process.
711 *Journal of Agricultural and Food Chemistry*, *70*(26), 8124-8133.
712 https://doi.org/10.1021/acs.jafc.2c01711

713 Chiang, J. H., Eyres, G. T., Silcock, P. J., Hardacre, A. K., & Parker, M. E. (2019a). Changes in the
714 physicochemical properties and flavour compounds of beef bone hydrolysates after
715 Maillard reaction. *Food Research International*, *123*, 642-649.
716 https://doi.org/https://doi.org/10.1016/j.foodres.2019.05.024

717 Chiang, J. H., Loveday, S. M., Hardacre, A. K., & Parker, M. E. (2019b). Effects of soy protein to
718 wheat gluten ratio on the physicochemical properties of extruded meat analogues.
719 *Food Structure*, *19*, 100102.
720 https://doi.org/https://doi.org/10.1016/j.foostr.2018.11.002

721 Chiang, J. H., Tay, W., Ong, D. S. M., Liebl, D., Ng, C. P., & Henry, C. J. (2021). Physicochemical,
722 textural and structural characteristics of wheat gluten-soy protein composited meat
723 analogues prepared with the mechanical elongation method. *Food Structure*, *28*,
724 100183. https://doi.org/https://doi.org/10.1016/j.foostr.2021.100183

725 Cutroneo, S., Prandi, B., Pellegrini, N., Sforza, S., & Tedeschi, T. (2024). Assessment of protein
726 quality and digestibility in plant-based meat analogues. *Journal of Agricultural and*
727 *Food Chemistry*, *72*(14), 8114-8125. https://doi.org/10.1021/acs.jafc.3c08956

728 Dai, H., & An, H. (2024). Effect of protease hydrolysis pretreatment on extruder response and
729 the structural characteristics of high-moisture plant-protein extrudates. *Journal of*
730 *Food Engineering*, *376*, 112062.
731 https://doi.org/https://doi.org/10.1016/j.jfoodeng.2024.112062

732 Day, L. (2013). Proteins from land plants – Potential resources for human nutrition and food
733 security. *Trends in Food Science & Technology*, *32*(1), 25-42.
734 https://doi.org/https://doi.org/10.1016/j.tifs.2013.05.005

735 Dent, T., Campanella, O., & Maleky, F. (2023). Enzymatic hydrolysis of soy and chickpea
736 protein with Alcalase and Flavourzyme and formation of hydrogen bond mediated
737 insoluble aggregates. *Current Research in Food Science*, *6*, 100487.
738 https://doi.org/https://doi.org/10.1016/j.crfs.2023.100487

739 Dou, W., Zhang, X., Zhao, Y., Zhang, Y., Jiang, L., & Sui, X. (2022). High moisture extrusion
740 cooking on soy proteins: Importance influence of gums on promoting the fiber

formation. *Food Research International*, *156*, 111189. https://doi.org/https://doi.org/10.1016/j.foodres.2022.111189

Dupont, D., Mandalari, G., Molle, D., Jardin, J., Léonil, J., Faulks, R. M., Wickham, M. S., Mills, E. N., & Mackie, A. R. (2010). Comparative resistance of food proteins to adult and infant in vitro digestion models. *Mol Nutr Food Res*, *54*(6), 767-780. https://doi.org/10.1002/mnfr.200900142

Egger, L., Schlegel, P., Baumann, C., Stoffers, H., Guggisberg, D., Brügger, C., Dürr, D., Stoll, P., Vergères, G., & Portmann, R. (2017). Physiological comparability of the harmonized INFOGEST in vitro digestion method to in vivo pig digestion. *Food Res Int*, *102*, 567-574. https://doi.org/10.1016/j.foodres.2017.09.047

Gu, M., Hong, T., Ma, Y., Xi, J., Zhao, Q., Xu, D., Jin, Y., Wu, F., & Xu, X. (2022). Effects of a commercial peptidase on rheology, microstructure, gluten properties of wheat dough and bread quality. *LWT*, *160*, 113266. https://doi.org/https://doi.org/10.1016/j.lwt.2022.113266

Guo, C., Zhao, X., Yang, Y., Li, M., & Yu, L. (2022). Effect of limited enzymatic hydrolysis on structural and functional properties of elaeagnus mollis oil meal protein. *Foods*, *11*(21), 3393. https://www.mdpi.com/2304-8158/11/21/3393

Gupta, R., Beg, Q., & Lorenz, P. (2002). Bacterial alkaline proteases: molecular approaches and industrial applications. *Applied Microbiology and Biotechnology*, *59*(1), 15-32. https://doi.org/10.1007/s00253-002-0975-y

He, X.-H., Liu, H.-Z., Zhao, G.-L., Wang, Q., & Chen, Q.-L. (2014). Effects of high pressure on the physicochemical and functional properties of peanut protein isolates. *Food Hydrocolloids*, *36*, 123–129. https://doi.org/10.1016/j.foodhyd.2013.08.031

Herreman, L., Nommensen, P., Pennings, B., & Laus, M. C. (2020). Comprehensive overview of the quality of plant- And animal-sourced proteins based on the digestible indispensable amino acid score. *Food Sci Nutr*, *8*(10), 5379-5391. https://doi.org/10.1002/fsn3.1809

Hua, X. Y., Long, Y., Ong, D. S. M., Theng, A. H. P., Shi, J. K., Osen, R., Wu, M., & Chiang, J. H. (2023). Mathematical optimisation of extruded mixed plant protein-based meat analogues based on amino acid compositions. *Current Research in Food Science*, *7*, 100648. https://doi.org/https://doi.org/10.1016/j.crfs.2023.100648

Hülsebusch, L., Heyn, T. R., Amft, J., & Schwarz, K. (2025). Extrusion of plant proteins: A review of lipid and protein oxidation and their impact on functional properties. *Food Chemistry*, *470*, 142607. https://doi.org/https://doi.org/10.1016/j.foodchem.2024.142607

Hwang, J., Son, W.-Y., Jeong, E. J., Kim, K.-S., Shin, E.-C., Song, D.-H., Lee, K.-W., & Kim, H.-W. (2025). Comparative exploration of antioxidant properties of alcalase- and trypsin-hydrolyzed porcine by-products and their classification for industrial use. *Applied Sciences*, *15*(1), 47. https://www.mdpi.com/2076-3417/15/1/47

Idowu, A. T., & Benjakul, S. (2019). Bitterness of fish protein hydrolysate and its debittering prospects. *Journal of Food Biochemistry*, *43*(9), e12978. https://doi.org/https://doi.org/10.1111/jfbc.12978

Kennedy, A. R. (1998). The Bowman-Birk inhibitor from soybeans as an anticarcinogenic agent123. *The American Journal of Clinical Nutrition*, *68*(6), 1406S-1412S. https://doi.org/https://doi.org/10.1093/ajcn/68.6.1406S

Khushairay, E. S. I., Ayub, M. K., & Babji, A. S. (2014). Effect of enzymatic hydrolysis of pancreatin and alcalase enzyme on some properties of edible bird's nest hydrolysate. *AIP Conference Proceedings*, *1614*(1), 427-432. https://doi.org/10.1063/1.4895235

Kumar, C. G., & Takagi, H. (1999). Microbial alkaline proteases: From a bioindustrial viewpoint. *Biotechnology Advances*, *17*(7), 561-594. https://doi.org/https://doi.org/10.1016/S0734-9750(99)00027-0

Lee, J.-S., Kim, S., Jeong, Y. J., Choi, I., & Han, J. (2023). Impact of interactions between soy and pea proteins on quality characteristics of high-moisture meat analogues prepared via extrusion cooking process. *Food Hydrocolloids*, *139*, 108567. https://doi.org/https://doi.org/10.1016/j.foodhyd.2023.108567

Li, Q., Chang, B., Huang, G., Wang, D., Gao, Y., Fan, Z., Sun, H., & Sui, X. (2025). Differential enzymatic hydrolysis: a study on its impact on soy protein structure, function, and soy milk powder properties. *Foods*, *14*(5), 906. https://www.mdpi.com/2304-8158/14/5/906

Lin, Q., Pan, L., Deng, N., Sang, M., Cai, K., Chen, C., Han, J., & Ye, A. (2022). Protein digestibility of textured-wheat-protein (TWP) -based meat analogues: (I) Effects of fibrous structure. *Food Hydrocolloids*, *130*, 107694. https://doi.org/https://doi.org/10.1016/j.foodhyd.2022.107694

López-Martínez, M. I., Toldrá, F., & Mora, L. (2024). Sequential enzymatic hydrolysis and ultrasound pretreatment of pork liver for the generation of bioactive and taste-related hydrolyzates. *Journal of Agricultural and Food Chemistry*, *72*(28), 15693-15703. https://doi.org/10.1021/acs.jafc.4c02362

Luz, A. B. S., de Medeiros, A. F., de Medeiros, G. C. B. S., Piuvezam, G., Passos, T. S., & Morais, A. H. d. A. (2024). Experimental protocols used to mimic gastrointestinal protein digestion: A systematic review. *Nutrients*, *16*(15), 2398. https://www.mdpi.com/2072-6643/16/15/2398

Maeda, H., Sakai, D., Kobayashi, T., Morita, H., Okamoto, A., Takeuchi, M., Kusumoto, K.-I., Amano, H., Ishida, H., & Yamagata, Y. (2016). Three extracellular dipeptidyl peptidases found in Aspergillus oryzae show varying substrate specificities. *Applied Microbiology and Biotechnology*, *100*(11), 4947-4958. https://doi.org/10.1007/s00253-016-7339-5

Meinlschmidt, P., Sussmann, D., Schweiggert-Weisz, U., & Eisner, P. (2016). Enzymatic treatment of soy protein isolates: effects on the potential allergenicity, technofunctionality, and sensory properties. *Food Science & Nutrition*, *4*(1), 11-23. https://doi.org/https://doi.org/10.1002/fsn3.253

Minekus, M., Alminger, M., Alvito, P., Ballance, S., Bohn, T., Bourlieu, C., Carrière, F., Boutrou, R., Corredig, M., Dupont, D., Dufour, C., Egger, L., Golding, M., Karakaya, S., Kirkhus, B., Le Feunteun, S., Lesmes, U., Macierzanka, A., Mackie, A., . . . Brodkorb, A. (2014). A standardised static in vitro digestion method suitable for food – an international consensus [10.1039/C3FO60702J]. *Food & Function*, *5*(6), 1113-1124. https://doi.org/10.1039/C3FO60702J

826 Mulet-Cabero, A.-I., Egger, L., Portmann, R., Ménard, O., Marze, S., Minekus, M., Le Feunteun,
827 S., Sarkar, A., Grundy, M. M. L., Carrière, F., Golding, M., Dupont, D., Recio, I., Brodkorb,
828 A., & Mackie, A. (2020). A standardised semi-dynamic in vitro digestion method
829 suitable for food – an international consensus [10.1039/C9FO01293A]. *Food &*
830 *Function*, *11*(2), 1702-1720. https://doi.org/10.1039/C9FO01293A

831 Nadeesha Dilrukshi, H. N., Torrico, D. D., Brennan, M. A., & Brennan, C. S. (2022). Effects of
832 extrusion processing on the bioactive constituents, in vitro digestibility, amino acid
833 composition, and antioxidant potential of novel gluten-free extruded snacks fortified
834 with cowpea and whey protein concentrate. *Food Chemistry*, *389*, 133107.
835 https://doi.org/https://doi.org/10.1016/j.foodchem.2022.133107

836 Nandan, A., & Nampoothiri, K. M. (2020). Therapeutic and biotechnological applications of
837 substrate specific microbial aminopeptidases. *Applied Microbiology and*
838 *Biotechnology*, *104*(12), 5243-5257. https://doi.org/10.1007/s00253-020-10641-9

839 Nourmohammadi, E., SadeghiMahoonak, A., Alami, M., & Ghorbani, M. (2017). Amino acid
840 composition and antioxidative properties of hydrolysed pumpkin (Cucurbita pepo L.)
841 oil cake protein. *International Journal of Food Properties*, *20*(12), 3244-3255.
842 https://doi.org/10.1080/10942912.2017.1283516

843 Ong, D. S. M., Hua, X. Y., Theng, A. H. P., Mutiargo, B., Lee, H. W., Osen, R., & Chiang, J. H.
844 (2025). Influence of mixed plant protein combinations on the physicochemical,
845 textural, structural and nutritional properties of extruded high-moisture meat
846 analogues. *Journal of Food Engineering*, *399*, 112633.
847 https://doi.org/https://doi.org/10.1016/j.jfoodeng.2025.112633

848 Orozco-Angelino, X., Espinosa-Ramírez, J., & Serna-Saldívar, S. O. (2023). Extrusion as a tool
849 to enhance the nutritional and bioactive potential of cereal and legume by-products.
850 *Food Research International*, *169*, 112889.
851 https://doi.org/https://doi.org/10.1016/j.foodres.2023.112889

852 Pismag, R., Polo, M., Hoyos, J., Bravo, J., & Roa, D. (2024). Effect of extrusion cooking on the
853 chemical and nutritional properties of instant flours. *F1000Research*, *12*(1356).
854 https://doi.org/10.12688/f1000research.140748.2

855 Rao, P. S., Bajaj, R., & Mann, B. (2020). Impact of sequential enzymatic hydrolysis on
856 antioxidant activity and peptide profile of casein hydrolysate. *J Food Sci Technol*,
857 *57*(12), 4562-4575. https://doi.org/10.1007/s13197-020-04495-2

858 Rathod, R. P., & Annapure, U. S. (2016). Effect of extrusion process on antinutritional factors
859 and protein and starch digestibility of lentil splits. *LWT - Food Science and Technology*,
860 *66*, 114-123. https://doi.org/https://doi.org/10.1016/j.lwt.2015.10.028

861 Rawlings, N. D., Barrett, A. J., & Bateman, A. (2012). MEROPS: the database of proteolytic
862 enzymes, their substrates and inhibitors. *Nucleic Acids Res*, *40*(Database issue), D343-
863 350. https://doi.org/10.1093/nar/gkr987

864 Razavizadeh, S., Alencikiene, G., Vaiciulyte-Funk, L., Ertbjerg, P., & Salaseviciene, A. (2022).
865 Utilization of fermented and enzymatically hydrolyzed soy press cake as ingredient for
866 meat analogues. *LWT*, *165*, 113736.
867 https://doi.org/https://doi.org/10.1016/j.lwt.2022.113736

Sá, A. G. A., Moreno, Y. M. F., & Carciofi, B. A. M. (2020). Food processing for the improvement of plant proteins digestibility. *Crit Rev Food Sci Nutr*, *60*(20), 3367-3386. https://doi.org/10.1080/10408398.2019.1688249

Sadowski, N., Talwar, R., Fischer, E. F., & Merritt, R. (2024). Generating demand for alternative protein in low- and middle- income countries: opportunities and experiences from nutritious and sustainable market solutions. *Current Developments in Nutrition*, *8*. https://doi.org/10.1016/j.cdnut.2023.101996

Santos-Sánchez, G., Miralles, B., Brodkorb, A., Dupont, D., Egger, L., & Recio, I. (2024). Current advances for in vitro protein digestibility. *Frontiers in Nutrition*, *Volume 11 - 2024*. https://doi.org/10.3389/fnut.2024.1404538

Sapatinha, M., Camacho, C., Pais-Costa, A. J., Fernando, A. L., Marques, A., & Pires, C. (2025). Enzymatic hydrolysis systems enhance the efficiency and biological properties of hydrolysates from frozen fish processing co-products. *Marine Drugs*, *23*(1), 14. https://www.mdpi.com/1660-3397/23/1/14

Schmid, E.-M., Farahnaky, A., Adhikari, B., & Torley, P. J. (2022). High moisture extrusion cooking of meat analogs: A review of mechanisms of protein texturization. *Comprehensive Reviews in Food Science and Food Safety*, *21*(6), 4573-4609. https://doi.org/https://doi.org/10.1111/1541-4337.13030

Schreuders, F. K. G., Dekkers, B. L., Bodnár, I., Erni, P., Boom, R. M., & van der Goot, A. J. (2019). Comparing structuring potential of pea and soy protein with gluten for meat analogue preparation. *Journal of Food Engineering*, *261*, 32-39. https://doi.org/https://doi.org/10.1016/j.jfoodeng.2019.04.022

Shahbal, N., Jing, X., Bhandari, B., Dayananda, B., & Prakash, S. (2023). Effect of enzymatic hydrolysis on solubility and surface properties of pea, rice, hemp, and oat proteins: Implication on high protein concentrations. *Food Bioscience*, *53*, 102515. https://doi.org/https://doi.org/10.1016/j.fbio.2023.102515

Singh, B. P., Paul, S., & Goel, G. (2024). Shotgun proteomics and molecular simulations on multifunctional bioactive peptides derived from the whey of unexplored “Gaddi” goat of Himalayas. *Food Chemistry*, *430*, 137075. https://doi.org/https://doi.org/10.1016/j.foodchem.2023.137075

Tacias-Pascacio, V. G., Morellon-Sterling, R., Siar, E.-H., Tavano, O., Berenguer-Murcia, Á., & Fernandez-Lafuente, R. (2020). Use of Alcalase in the production of bioactive peptides: A review. *International Journal of Biological Macromolecules*, *165*, 2143-2196. https://doi.org/https://doi.org/10.1016/j.ijbiomac.2020.10.060

Taghian Dinani, S., van der Harst, J. P., Boom, R., & van der Goot, A. J. (2023). Effect of l-cysteine and l-ascorbic acid addition on properties of meat analogues. *Food Hydrocolloids*, *134*, 108059. https://doi.org/https://doi.org/10.1016/j.foodhyd.2022.108059

Torcello-Gómez, A., Dupont, D., Jardin, J., Briard-Bion, V., Deglaire, A., Risse, K., Mechoulan, E., & Mackie, A. (2020). The pattern of peptides released from dairy and egg proteins is highly dependent on the simulated digestion scenario [10.1039/D0FO00744G]. *Food & Function*, *11*(6), 5240-5256. https://doi.org/10.1039/D0FO00744G

van der Velden, V. H., & Hulsmann, A. R. (1999). Peptidases: structure, function and modulation of peptide-mediated effects in the human lung. *Clin Exp Allergy*, *29*(4), 445-456. https://doi.org/10.1046/j.1365-2222.1999.00462.x

Vogelsang-O'Dwyer, M., Sahin, A. W., Arendt, E. K., & Zannini, E. (2022). Enzymatic hydrolysis of pulse proteins as a tool to improve techno-functional properties. *Foods*, *11*(9), 1307. https://www.mdpi.com/2304-8158/11/9/1307

Vogelsang-O'Dwyer, M., Sahin, A. W., Bot, F., O'Mahony, J. A., Bez, J., Arendt, E. K., & Zannini, E. (2023). Enzymatic hydrolysis of lentil protein concentrate for modification of physicochemical and techno-functional properties. *European Food Research and Technology*, *249*(3), 573-586. https://doi.org/10.1007/s00217-022-04152-2

Wang, Q., Sun, X., Tang, Z., Cao, Y., Yu, H., & Wu, M. (2025). Enhancing the physical and oxidative stability of hempseed protein emulsion via comparative enzymolysis with different proteases: Interfacial properties of the adsorption layer. *Food Research International*, *201*, 115654. https://doi.org/https://doi.org/10.1016/j.foodres.2024.115654

Wang, R., Edrington, T. C., Storrs, S. B., Crowley, K. S., Ward, J. M., Lee, T. C., Liu, Z. L., Li, B., & Glenn, K. C. (2017). Analyzing pepsin degradation assay conditions used for allergenicity assessments to ensure that pepsin susceptible and pepsin resistant dietary proteins are distinguishable. *PLOS ONE*, *12*(2), e0171926. https://doi.org/10.1371/journal.pone.0171926

Wang, W. (2005). Protein aggregation and its inhibition in biopharmaceutics. *International Journal of Pharmaceutics*, *289*(1), 1-30. https://doi.org/https://doi.org/10.1016/j.ijpharm.2004.11.014

Wang, X., Cheng, L., Wang, H., & Yang, Z. (2022). Limited Alcalase hydrolysis improves the thermally-induced gelation of quinoa protein isolate (QPI) dispersions. *Curr Res Food Sci*, *5*, 2061-2069. https://doi.org/10.1016/j.crfs.2022.10.027

Webb, D., Dogan, H., Li, Y., & Alavi, S. (2023). Physico-chemical properties and texturization of pea, wheat and soy proteins using extrusion and their application in plant-based meat. *Foods*, *12*(8), 1586. https://www.mdpi.com/2304-8158/12/8/1586

Wittek, P., Walther, G., Karbstein, H. P., & Emin, M. A. (2021). Comparison of the rheological properties of plant proteins from various sources for extrusion applications. *Foods*, *10*(8), 1700. https://www.mdpi.com/2304-8158/10/8/1700

Woo Choi, H., Ryoo, C., Hahn, J., & Choi, Y. J. (2023). Development of a novel technology for high-moisture textured soy protein using a vacuum packaging and pressurized heat (vacuum-autoclaving) treatment. *Food Chemistry*, *399*, 133887. https://doi.org/https://doi.org/10.1016/j.foodchem.2022.133887

Wouters, A. G. B., Rombouts, I., Fierens, E., Brijs, K., & Delcour, J. A. (2016). Relevance of the functional properties of enzymatic plant protein hydrolysates in food systems. *Comprehensive Reviews in Food Science and Food Safety*, *15*(4), 786-800. https://doi.org/https://doi.org/10.1111/1541-4337.12209

Xia, S., Xue, Y., Xue, C., Jiang, X., & Li, J. (2022). Structural and rheological properties of meat analogues from Haematococcus pluvialis residue-pea protein by high moisture

952 extrusion. *LWT*, *154*, 112756.
953 https://doi.org/https://doi.org/10.1016/j.lwt.2021.112756

954 Xin, M., Zhao, M., Tian, J., & Li, B. (2023). Guidelines for in vitro simulated digestion and
955 absorption of food. *Food Frontiers*, *4*(1), 524-532.
956 https://doi.org/https://doi.org/10.1002/fft2.186

957 Zhang, B., Liu, G., Ying, D., Sanguansri, L., & Augustin, M. A. (2017). Effect of extrusion
958 conditions on the physico-chemical properties and in vitro protein digestibility of
959 canola meal. *Food Research International*, *100*, 658-664.
960 https://doi.org/https://doi.org/10.1016/j.foodres.2017.07.060

961 Zhang, L., Sun, X., Lu, X., Wei, S., Sun, Q., Jin, L., Song, G., You, J., & Li, F. (2022).
962 Characterization of peanut protein hydrolysate and structural identification of umami-
963 enhancing peptides. *Molecules*, *27*(9), 2853. https://www.mdpi.com/1420-
964 3049/27/9/2853

965 Zhang, T., Yu, S., Pan, Y., Li, H., Liu, X., & Cao, J. (2023). Properties of texturized protein and
966 performance of different protein sources in the extrusion process: A review. *Food*
967 *Research International*, *174*, 113588.
968 https://doi.org/https://doi.org/10.1016/j.foodres.2023.113588

969 Zhou, Q.-C., Liu, N., & Feng, C.-X. (2017). Research on the effect of papain co-extrusion on pea
970 protein and enzymolysis antioxidant peptides. *Journal of Food Processing and*
971 *Preservation*, *41*(6), e13301. https://doi.org/https://doi.org/10.1111/jfpp.13301

972 Zhu, P., Yang, J., & Chen, L. (2024). Chapter 6 - Protein–water–protein interaction: viscosity
973 and gelation. In J. P. D. Wanasundara, C. Schmitt, & B. P. Lamsal (Eds.), *Functionality*
974 *of Plant Proteins* (pp. 115-150). Academic Press.
975 https://doi.org/https://doi.org/10.1016/B978-0-323-91721-6.00005-0

976

Tables

Table 1 Physicochemical and textural properties of high-moisture meat analogues treated with different enzymes during extrusion.

Enzyme	Concentration (% w/w)	Physicochemical properties		Textural properties			
		Protein content (%)	pH	Hardness (N)	Springiness	Chewiness (N)	Degree of texturisation
No enzyme (MANE)	0	35.27 ± 0.39 ^{ab}	7.32 ± 0.05 ^{de}	198.91 ± 18.36 ^{a}	0.92 ± 0.02 ^{a}	140.32 ± 20.51 ^{a}	1.18 ± 0.08 ^{abc}
Flavourzyme®, FL (MAF)	0.5	32.18 ± 0.99 ^{cde}	7.44 ± 0.01 ^{ab}	161.51 ± 16.17 ^{bc}	0.89 ± 0.03 ^{a}	108.38 ± 15.23 ^{bc}	1.37 ± 0.27 ^{ab}
	1.0	32.89 ± 0.29 ^{abcde}	7.42 ± 0.01 ^{abc}	169.44 ± 11.36 ^{bc}	0.91 ± 0.01 ^{a}	114.77 ± 8.23 ^{b}	1.52 ± 0.21 ^{a}
	2.5	33.12 ± 0.67 ^{abcd}	7.18 ± 0.02 ^{f}	158.83 ± 3.57 ^{bc}	0.88 ± 0.04 ^{ab}	99.94 ± 7.41 ^{bc}	1.37 ± 0.17 ^{ab}
	5.0	33.13 ± 0.71 ^{abcd}	6.96 ± 0.02 ^{h}	159.36 ± 14.33 ^{bc}	0.85 ± 0.04 ^{ab}	90.04 ± 6.63 ^{c}	1.24 ± 0.10 ^{ab}
Protana® Prime, PP (MAP)	0.5	30.29 ± 1.32 ^{e}	7.47 ± 0.02 ^{a}	156.68 ± 8.45 ^{c}	0.91 ± 0.06 ^{a}	104.95 ± 9.71 ^{bcde}	1.24 ± 0.32 ^{ab}
	1.0	32.36 ± 0.25 ^{cde}	7.38 ± 0.02 ^{bcd}	182.68 ± 17.35 ^{ab}	0.88 ± 0.05 ^{ab}	121.53 ± 13.80 ^{ab}	1.34 ± 0.17 ^{ab}
	2.5	32.56 ± 0.40 ^{bcde}	7.41 ± 0.01 ^{abc}	168.68 ± 8.87 ^{bc}	0.89 ± 0.02 ^{ab}	112.01 ± 6.16 ^{b}	1.09 ± 0.17 ^{bc}
	5.0	32.94 ± 0.17 ^{abcde}	7.35 ± 0.01 ^{cde}	170.02 ± 8.32 ^{bc}	0.90 ± 0.05 ^{a}	113.72 ± 16.22 ^{b}	1.06 ± 0.06 ^{bc}
Alcalase®, AL (MAA)	0.5	35.64 ± 0.02 ^{a}	7.41 ± 0.04 ^{abc}	162.94 ± 12.67 ^{bc}	0.88 ± 0.02 ^{ab}	103.94 ± 9.80 ^{bc}	1.41 ± 0.29 ^{ab}
	1.0	33.73 ± 0.05 ^{abc}	7.30 ± 0.04 ^{e}	179.60 ± 17.85 ^{abc}	0.87 ± 0.02 ^{ab}	111.91 ± 13.57 ^{bc}	1.05 ± 0.09 ^{bc}

	2.5	32.61 ± 0.20 ^{bcde}	7.16 ± 0.04 ^{f}	91.99 ± 7.906 ^{d}	0.78 ± 0.08 ^{b}	35.91 ± 5.90 ^{d}	0.87 ± 0.13 ^{c}
	5.0	30.56 ± 2.63 ^{de}	7.08 ± 0.03 ^{g}	74.08 ± 4.39 ^{d}	0.64 ± 0.14 ^{c}	21.58 ± 7.74 ^{d}	0.84 ± 0.08 ^{c}

Data are presented as the mean and standard deviation of three replicates. Values bearing different lowercase letters on each column were significantly different ($p \leq 0.05$) according to Tukey's post-hoc test.

Table 2 Free amino acid released from digested HMMA co-extruded with 1% w/w enzyme concentrations (i.e., no enzyme added (MANE), Flavourzyme® (MAF), Protana® Prime (MAP) and Alcalase® (MAF)).

Free amino acid	Concentration (mg/g protein)			
	MANE	MAF-1%	MAP-1%	MAA-1%
Indispensable AA (IAA)				
Histidine	1.03 ± 0.06 [b]	8.12 ± 0.28 [a]	7.82 ± 0.59 [a]	6.79 ± 0.58 [a]
Isoleucine	3.31 ± 0.13 [b]	14.72 ± 0.51 [a]	14.13 ± 1.05 [a]	12.07 ± 1.04 [a]
Leucine	12.12 ± 0.42 [b]	41.56 ± 1.43 [a]	41.20 ± 3.02 [a]	35.62 ± 3.09 [a]
Lysine	10.98 ± 0.42 [c]	36.97 ± 1.28 [ab]	40.27 ± 3.01 [a]	32.83 ± 2.82 [b]
Methionine	1.79 ± 0.06 [b]	8.03 ± 0.28 [a]	8.41 ± 0.61 [a]	6.96 ± 0.60 [a]
Phenylalanine	11.45 ± 0.37 [b]	35.40 ± 1.22 [a]	38.99 ± 2.80 [a]	31.77 ± 2.77 [a]
Threonine	1.16 ± 0.08 [b]	9.36 ± 0.33 [a]	8.88 ± 0.70 [a]	7.68 ± 0.65 [a]
Valine	2.86 ± 0.13 [b]	14.49 ± 0.50 [a]	13.91 ± 1.06 [a]	11.92 ± 1.02 [a]
Total IAA	44.70 ± 1.68 [b]	168.65 ± 5.83 [a]	173.61 ± 12.84 [a]	145.64 ± 12.56 [a]
Dispensable AA (DAA)				
Alanine	1.62 ± 0.10 [b]	10.33 ± 0.36 [a]	9.84 ± 0.78 [a]	8.49 ± 0.71 [a]
Arginine	23.65 ± 0.84 [c]	45.50 ± 1.58 [ab]	54.41 ± 4.10 [a]	41.99 ± 3.57 [b]
Aspartic acid	0.49 ± 0.05 [b]	3.88 ± 0.14 [a]	4.12 ± 0.35 [a]	3.33 ± 0.27 [a]
Cysteine*	3.79 ± 0.15 [b]	13.93 ± 0.48 [a]	14.84 ± 1.11 [a]	12.37 ± 1.06 [a]
Glutamic acid	2.96 ± 0.20 [b]	18.52 ± 0.65 [a]	17.74 ± 1.44 [a]	15.10 ± 1.26 [a]
Glycine	0.85 ± 0.10 [b]	8.60 ± 0.31 [a]	9.13 ± 0.78 [a]	7.96 ± 0.65 [a]
Proline	1.05 ± 0.08 [b]	1.49 ± 0.05 [a]	0.76 ± 0.05 [b]	0.97 ± 0.08 [ab]
Serine	0.84 ± 0.08 [b]	7.82 ± 0.28 [a]	7.18 ± 0.60 [a]	6.24 ± 0.51 [a]
Tyrosine*	3.39 ± 0.19 [b]	15.08 ± 0.53 [a]	17.24 ± 1.37 [a]	15.99 ± 1.88 [a]

Total DAA	38.65 ± 1.79 [b]	125.17 ± 4.37 [a]	135.25 ± 10.58 [a]	112.43 ± 4.19 [a]
Total FAA	83.34 ± 3.47 [b]	293.82 ± 10.20 [a]	308.86 ± 23.43 [a]	286.99 ± 22.12 [a]

* Cysteine & Tyrosine are conditionally indispensable.

Data are presented as the mean and standard deviation. Values bearing different lowercase letters on each column were significantly different ($p \leq 0.05$) according to Tukey's post-hoc test.

Figures

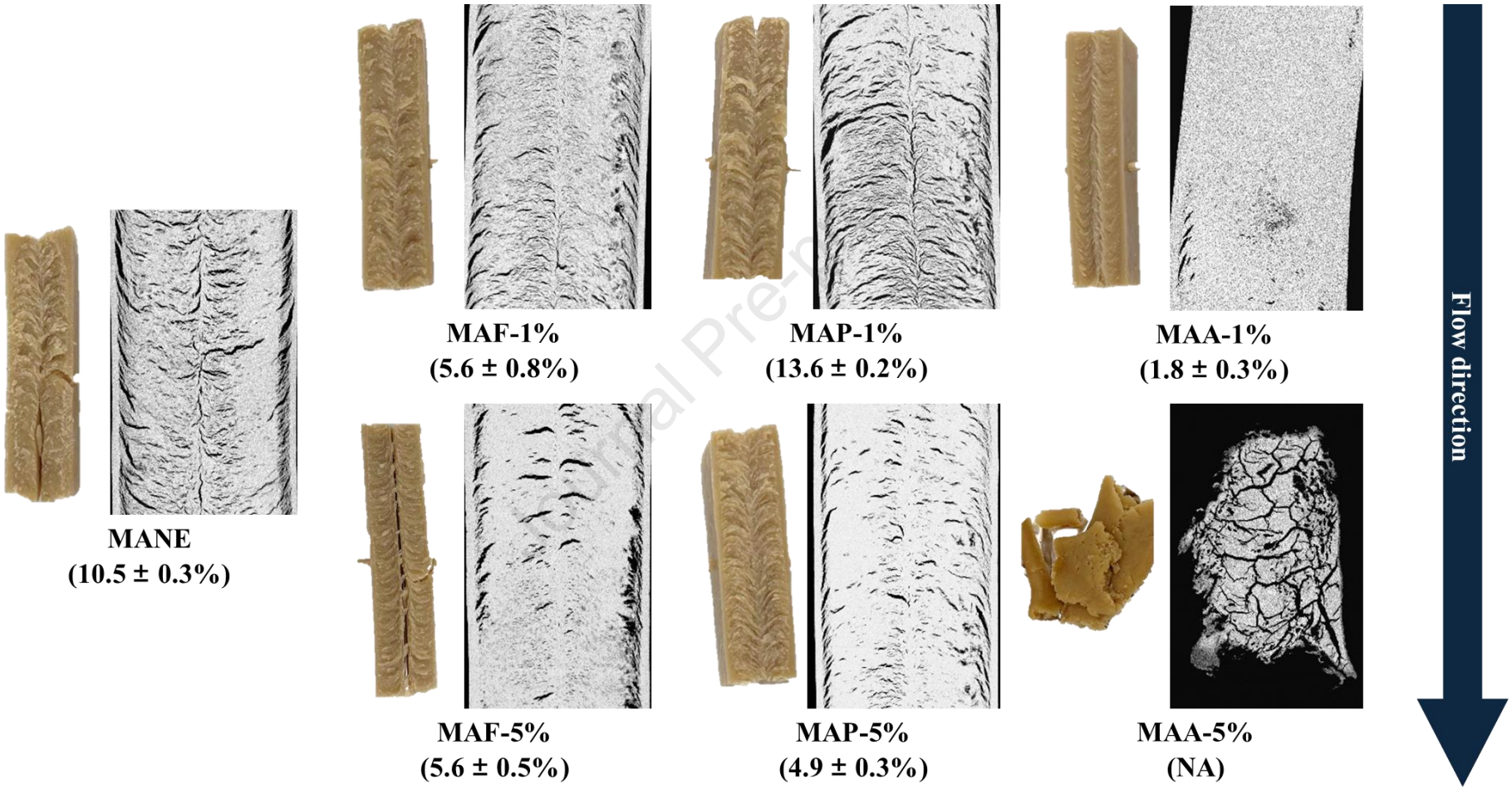
MANE
(10.5 ± 0.3%)
MAF-1%
(5.6 ± 0.8%)
MAP-1%
(13.6 ± 0.2%)
MAA-1%
(1.8 ± 0.3%)
MAF-5%
(5.6 ± 0.5%)
MAP-5%
(4.9 ± 0.3%)
MAA-5%
(NA)
Flow direction

Figure 1 Visual and X-ray computed tomography (XCT) images of the longitude cross-section of high-moisture meat analogues treated with different enzymes and concentrations and their porosity expressed as (mean ± standard deviation); no enzyme added (MANE), Flavourzyme® at 1 and 5% w/w (MAF), Protana® Prime at 1 and 5% w/w (MAP), and Alcalase® at 1 and 5% w/w (MAA).

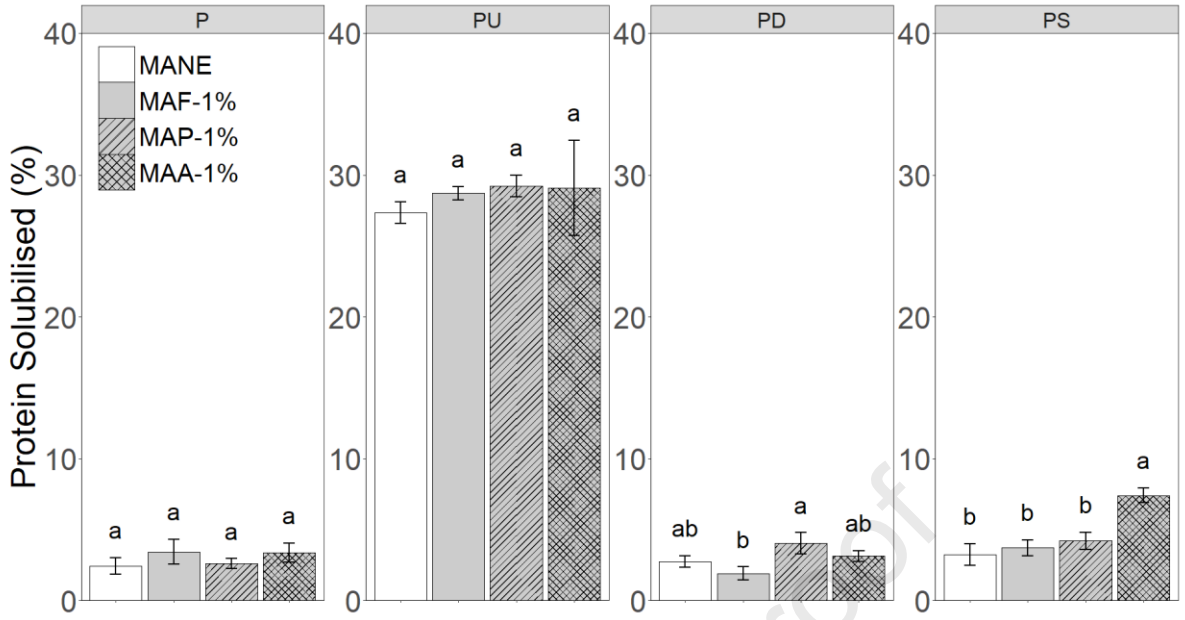

Figure 2 Protein solubilised with different extracting solutions for HMMA co-extruded with increasing enzyme concentrations (i.e., no enzyme added (MANE), Flavourzyme® (MAF), Protana® Prime (MAP) and Alcalase® (MAF) at 1% w/w) during extrusion. Data are presented as the mean of triplicate, and error bars are the standard deviation. Different alphabets (a, b, c) within each extracting solution are significantly different from each other (p<0.05).

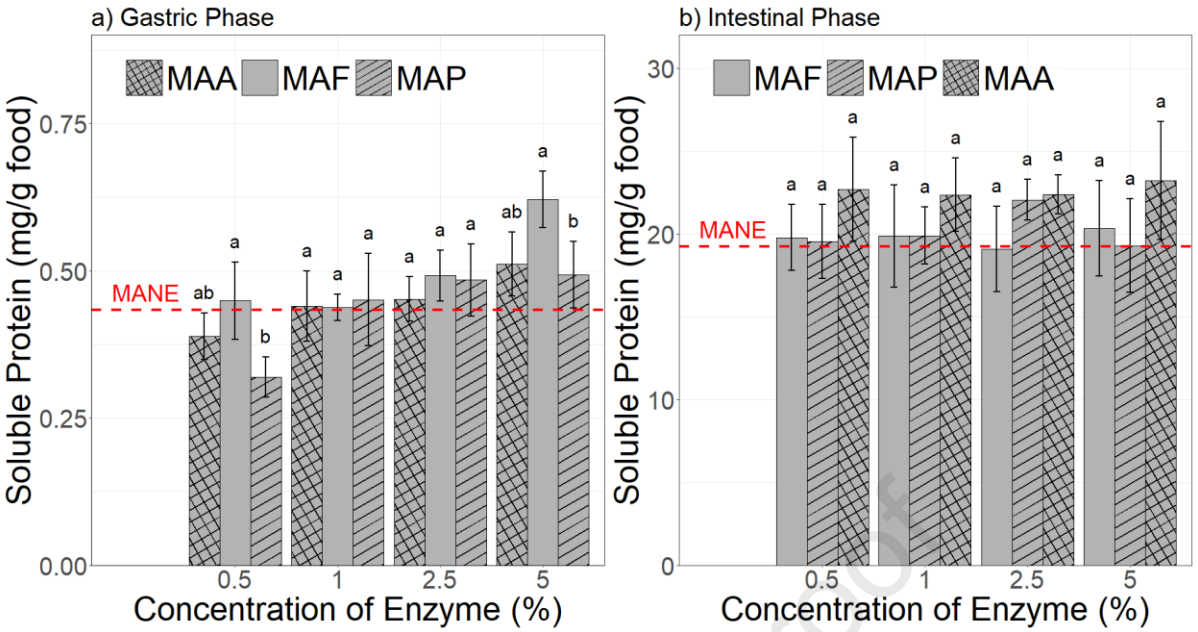

Figure 3 Soluble protein in (a) gastric digesta and (b) intestinal digesta of HMMA co-extruded with increasing enzyme (0.5, 1, 2.5 and 5%) concentrations (i.e., no enzyme added (MANE), Flavourzyme® (MAF), Protana® Prime (MAP) and Alcalase® (MAF)). Data are presented as the mean of triplicate, and error bars are the standard deviation. Different alphabets (a, b, c) within each enzyme concentration are significantly different from each other (p<0.05, using Tukey's post hoc test).

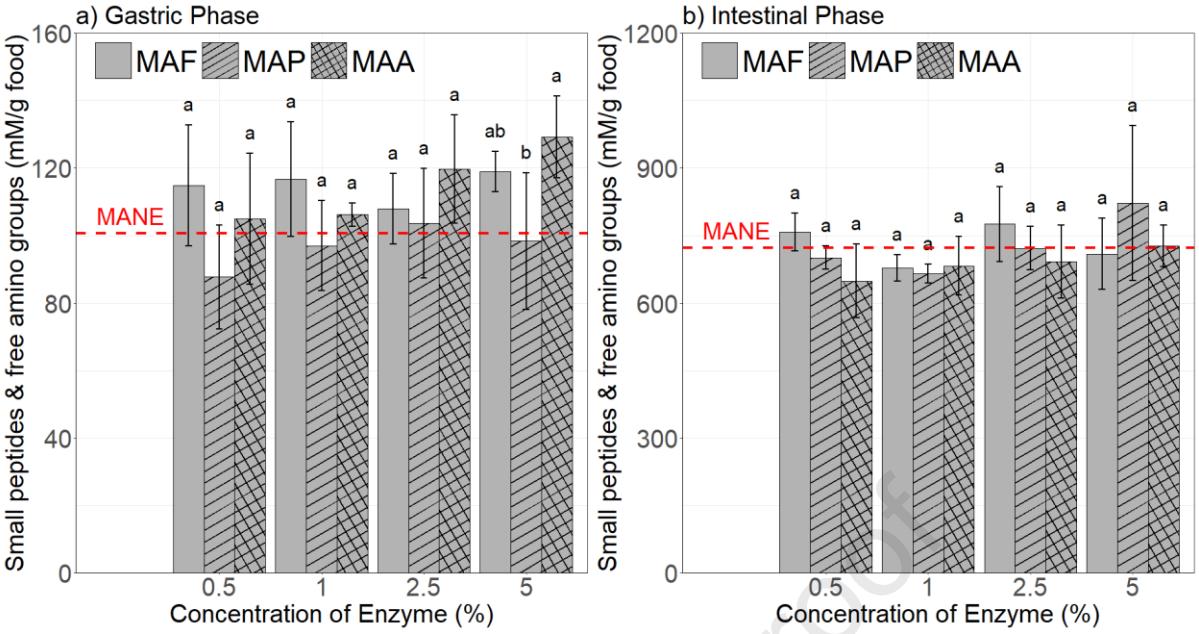

Figure 4 Small peptides (approximately <6 kDa) and free amino groups in the (a) gastric digesta and (b) intestinal digesta of HMMA co-extruded with increasing enzyme (0.5, 1, 2.5 and 5%) concentrations (i.e., no enzyme added (MANE), Flavourzyme® (MAF), Protana® Prime (MAP) and Alcalase® (MAF)). Data are presented as the mean of triplicate, and error bars are the standard deviation. Different alphabets (a, b, c) within each enzyme concentration are significantly different from each other (p<0.05, using Tukey's post hoc test).

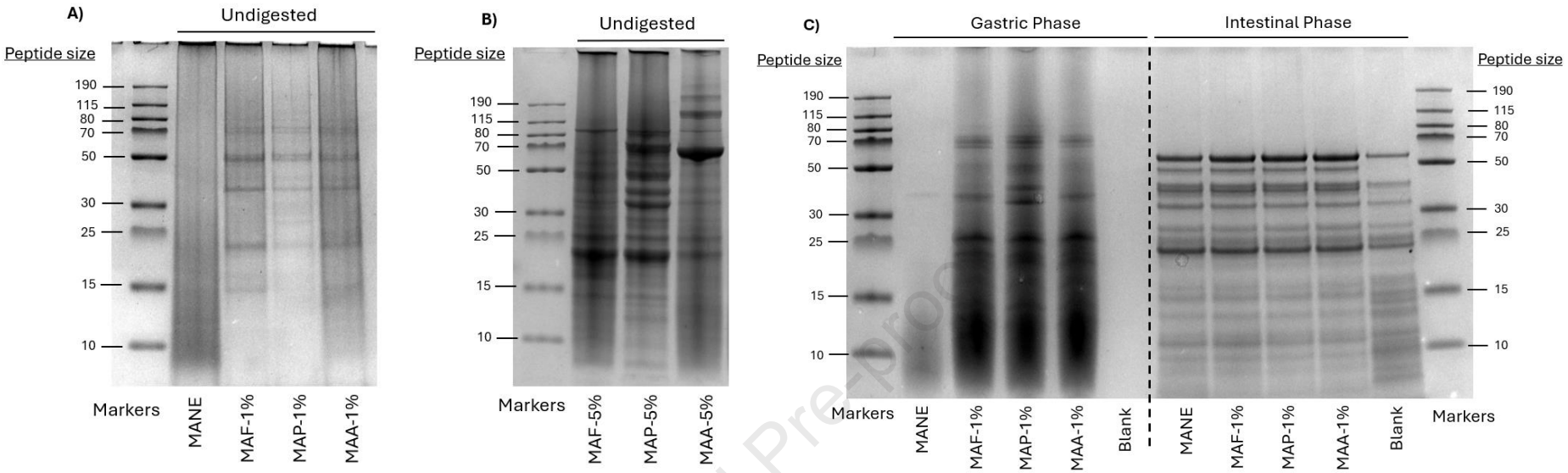

Figure 5 SDS-PAGE showing the protein profile of (**a**) undigested HMMA at 1% enzyme concentration, (**b**) undigested HMMA at 5% enzyme concentration, and (**c**) digested HMMA with blank markers. **5a** – Lane 1: protein molecular weight marker (kDa); Lane 2 – 5: undigested HMMA (MANE, MAF-1%, MAP-1%, MAA-1%, respectively). **5b** – Lane 1: protein molecular weight marker (kDa); Lane 2 – 4: undigested HMMA (MAF-5%, MAP-5%, MAA-5%, respectively). **5c** – Lane 1 & 12: protein molecular weight marker (kDa); Lane 2 - 6: gastric digesta of HMMA (MANE, MAF-1%, MAP-1%, MAA-1%, gastric blank, respectively); Lane 7 - 11: intestinal digesta of HMMA (MANE, MAF-1%, MAP-1%, MAA-1%, intestinal blank, respectively).

Highlights

- Low-to-moderate enzyme concentrations (0.5-1% w/w) improved texture of HMMA.
- High enzyme concentrations negatively impacted texture of HMMA.
- Enzyme treatments significantly increased protein digestibility of HMMA.
- Enzyme type altered protein solubility and yielded unique peptide profiles.
- Enzyme type influenced the free amino acid profile of HMMA.

Declaration of interests

☒ The authors declare that they have no known competing financial interests or personal relationships that could have appeared to influence the work reported in this paper.

☐The authors declare the following financial interests/personal relationships which may be considered as potential competing interests: